www.ietdl.org

Published in IET Science, Measurement and Technology
Received on 29th April 2010
Revised on 12th August 2010
doi: 10.1049/iet-smt.2010.0051

ISSN 1751-8822

Performance of time-difference-of-arrival ultra wideband indoor localisation

J. Xu M. Ma C.L. Law

School of Electrical and Electronic Engineering, Nanyang Technological University, Singapore
E-mail: xujun1023@hotmail.com

Abstract: Ultra wideband (UWB) is a good candidate for indoor positioning, thanks to its ability to resolve multipath and penetrate through walls. This study investigates the performance of UWB-based time difference of arrival (TDOA) positioning for indoor environment, where one or more blind nodes are to be localised with the aid of a number of anchor nodes. The positions of the blind nodes are estimated using the previously proposed iterative localisation method. The achievable positioning accuracy is analysed in terms of Cramer–Rao lower bound (CRLB), which is a theoretical lower bound on the variance of the positions of blind nodes. The range errors are modelled as distance independent (DI) and distance dependent (DD) for line-of-sight (LOS) and non-line-of-sight (NLOS) cases. Closed-form expressions of CRLB for TDOA localisation are derived and the theoretical analyses have been verified by experimental results.

1 Introduction

Ultra wideband (UWB) technology is a high-bandwidth communication scheme which offers several advantages for position localisation [1, 2]. The bandwidth of UWB signals is of the order of several gigahertzs, which corresponds to sub-nanosecond time resolution. As a result of the fine time resolution, UWB transmissions are well suited for precise positioning using time domain techniques. The characteristic of short pulse duration allows the receiver to differentiate and resolve the different multipath components of the arrival signals. This provides robustness against multipath fading and it makes UWB particularly attractive for indoor position localisation [3–5]. In addition, the wide bandwidth of the UWB signals results in very low-power spectral densities, which reduces interference on other radio-frequency (RF) systems. Global positioning system (GPS) is the most recognised and widely used positioning system. However, GPS is not suitable for indoor environments because GPS signals cannot penetrate through walls.

So far, most UWB positioning systems use a time-based method for ranging, whereas time difference of arrival (TDOA) is one of the commonly used ranging techniques. TDOA estimates the difference of the arrival time of the signals between the synchronised anchor nodes. It does not require knowledge of the absolute time of the transmission, and therefore only synchronicity of the anchor nodes is necessary for TDOA-based positioning. Each TDOA range determines a hyperbola, and the intersection point of the two hyperbolas is the estimated location of the blind node. Different positioning algorithms can be applied to estimate the positions of the interested nodes after obtaining the ranges [6–9].

The localisation accuracy depends mainly on four factors: (i) Accuracy of the range measurements: The range measurements used for the position estimations can be corrupted by multipath or non-line-of-sight (NLOS), which cause the range estimations to be noisy or biased. The localisation performance can be severely degraded by poor range measurements. (ii) Location errors of the anchor nodes: As mentioned earlier, the time resolution of UWB ranging is in sub-nanosecond, and the corresponding range measurements are on the order of centimetres. If the locations of anchor nodes are not accurate enough, the location errors of the anchor nodes may become a dominant source of positioning error. Therefore the precision of the locations of the anchor nodes also play an important role in UWB localisation system. (iii) Geometric configuration of the system: Geometric configuration refers how the anchor nodes are placed relative to the blind nodes, which will be investigated in details in the following sections. (iv) Positioning algorithm used to estimate the location of a blind node: Without a robust positioning algorithm, the blind node may not be successfully localised in indoor environment. There also exist trade-offs among the positioning accuracy, computational complexity, cost and power consumption. In this paper, we focus on the effects induced by the ranging accuracy and the geometric configuration, and thus it is assumed that the anchor nodes are perfectly placed, and one positioning algorithm is used to determine the locations of the blind nodes.

The performance of the localisation can be evaluated using Cramer–Rao lower bound (CRLB) [8, 10–14]. CRLB is a theoretical lower bound of the variance of the position estimations and shows the smallest positioning error that can be achieved. It is defined as the inverse of the Fisher information matrix (FIM) [10]. In [8], CRLB for

line-of-sight (LOS) TDOA localisation has been derived and compared with the achievable accuracy of various position localisation algorithms. Position estimation bounds for localisation of sensors in a sensor network, either with or without anchor nodes, have been derived in [12]. The effects of geometric configurations and node density on the localisation accuracy have been investigated in [13]. In [14], Shen *et al.* have applied the notion of equivalent FIM to simplify the individual ranging information and discussed the fundamental limits of cooperative localisation. However, these discussions concentrate on LOS situations, and do not take the multipath issue and NLOS case into account. Furthermore, the existing solutions have not paid much attention on the special characteristics of the UWB pulse. In this paper, we will provide a systematic analysis of TDOA UWB localisation accuracy with consideration above issues in order to enhance the results of current existing investigations. For simplicity, we restrict ourselves to two dimensions only. However, the results can be easily extended to three dimensions.

The objective of this paper is to investigate the performance of the UWB-based positioning. We model the measurement errors for UWB ranging and derive the closed-form expressions of the theoretical lower bounds for TDOA-based localisation. We compare the theoretical lower bounds with actual measurements for distance-dependent (DD) range errors and distance-independent (DI) range errors. Some numerical results of the lower bounds are also discussed.

The remainder of the paper is organised as follows. Section 2 describes the methodology to model the range errors and derives the theoretical lower bounds of the positioning. Section 3 provides the experimental results to verify the theoretical analyses, and Section 4 presents some concluding remarks.

2 Fundamental limits for UWB TDOA localisation

2.1 Range error modelling

Consider a network where all the anchor nodes are synchronised. The anchor nodes measure the TDOA of the signals, and the time differences are then converted to range measurements. Two sources of errors in range estimations are distinguished. The first source of errors is the standard system measurement noise, modelled as a zero-mean random variable. The second type of errors is the NLOS error, a product of the reflection of the signals when the LOS path is obstructed. Since a reflected path is longer than the LOS path, the NLOS error produces a positive bias in distance measurements.

In LOS propagation, the range errors are usually modelled as zero-mean Gaussian, which is caused by the measurement system itself. Therefore we can model the TDOA ranges in LOS propagation as

$$r_{m,k} = d_{m,k} + n_{m,k} \tag{1}$$

where $r_{m,k}$ are measured TDOA ranges between the anchor nodes and the querying blind node *i*. d represents the actual distance and $n(t)$ is Gaussian measurement noise.

The transmitted time hopping impulse response (TH-IR) UWB signal is given by [4]

$$s(t) = \sum_{j=-\infty}^{+\infty} d_j b_{\lfloor j/N_f \rfloor} w(t - jT_f - c_j^k T_c) \tag{2}$$

where d_j represents the polarity and takes values ± 1, b is the information symbol transmitted, $w(t)$ is a monocycle, T_f is the average pulse repetition time, $\{c_j\}$ is a pseudo-random sequence assigned to each user k, T_c is chip interval and N_f represents the processing gain.

A simple UWB multipath channel model is used. It assumes that signals arrive at the receiver with different amplitudes, phases and delays, and hence the received signal is a linear combination of replicas of the single-path signal with different delays and amplitudes

$$\begin{aligned} r(t) &= a_0 s(t - \tau_0) + \sum_{i=1}^{L} a_i s(t - \tau_i) + n(t) \\ &= \sum_{i=0}^{L} a_i s(t - \tau_i) + n(t) \end{aligned} \tag{3}$$

where $r(t)$ is the received signal. α_0 and τ_0 are the direct path amplitude and propagation delay. α_i and τ_i are the amplitude and propagation delay of the ith multipath, respectively. L is the number of multipaths. $n(t)$ is the white Gaussian noise.

The arrival time can be estimated using the maximum likelihood (ML) estimator. It has been derived that the theoretical bound of time of arrival (TOA) for a single path is [10]

$$\sigma_{\text{toa}}^2 \geq \frac{c^2}{2\ \text{SNR}\ \overline{F^2}} \tag{4}$$

where

$$\overline{F^2} = \frac{\int_{-\infty}^{\infty} (2\pi F)^2 |S(F)|^2\, \mathrm{d}F}{\int_{-\infty}^{\infty} |S(F)|^2\, \mathrm{d}F}$$

is the mean square bandwidth. $\text{SNR} = E_b/N_o$, represents the signal-to-noise ratio. c is the speed of light.

As we can see from (4), the variance of the TOA ranges is inversely proportional to SNR, which is intuitively reasonable since the stronger signals can be detected easier. The inequality also shows that the TOA accuracy increases with the bandwidth, which makes UWB a good candidate for time-based ranging. We know that the TDOA can be regarded as the difference between two TOA measurements. Assuming the two TOAs are uncorrelated, and the variance of TDOA measurement is

$$\text{var}[r_{m,k}] = \text{var}[r_m] + \text{var}[r_k] \tag{5}$$

where var[·] is the variance of a random variable.

Thus, we can obtain the bound of the TDOA measurement

$$\sigma_{\text{tdoa}}^2 = 2\sigma_{\text{toa}}^2 \geq \frac{c^2}{\text{SNR}\ \overline{F^2}} \tag{6}$$

and it is obvious that the accuracy of TDOA measurements also increases with bandwidth and strength of the signals.

Therefore the range errors in additive white Gaussian noise (AWGN) channel can be modelled as

$$(r_{m,k} - d_{m,k}) \sim N(0, \sigma^2_{m,k}) \tag{7}$$

where $\sigma^2_{m,k}$ is the variance, and its bound satisfies (4).

In the above discussion, it is assumed that the range errors are independent of the actual distances between the transmitters and receivers. It is reasonable for an open area without many reflections. The mean and variance of the Gaussian errors are the same for different ranges in the same area. However, in a dense multipath environment, a range error increases as the actual range increases [16]. This is reasonable because, intuitively, there are more reflected paths as the range increases, which make detecting the first path more difficult. Similar to the DI range error case, we find the variance of TDOA range error from TOA. The variance of the range-dependent TOA range errors can be modelled as

$$\sigma^2_{\text{toa}}(d_i) = \sigma^2_0 d_i^{\alpha} \tag{8}$$

where σ^2_0 is the variance of the TOA measurement at 1 m distance, and α is the exponent that describes the ranging accuracy decay with increase of distance. It should be noted α is not exactly equal to the path loss exponent n, although its value is related to the path loss exponent. The path loss exponent indicates the rate at which the path loss increases with distance. The value of path loss exponent depends on the specific propagation environment. Path loss may be due to many effects, such as free-space loss, refraction, diffraction, reflection etc. Path loss is the reason of range error increasing with distance. We can represent α in terms of the path loss exponent as

$$\alpha = \lambda n \tag{9}$$

where λ is a coefficient used to accommodate the increase pace of ranging error below linear, and its value is less than 1. Then we can obtain the variance for TDOA

$$\sigma^2_{\text{tdoa}}(d_{m,n}) = \sigma^2_0(d_m^{\alpha} + d_k^{\alpha}) \tag{10}$$

It should be noted that the accuracies of the two TOAs are no longer same, because the accuracy is dependent on the distance.

If there is no LOS between two nodes, the signal will travel an extra distance resulting in extra time of propagation. A positive bias is then introduced into the measurement due to the delay of the received signal, because the LOS between two nodes has been blocked, and hence the NLOS TDOA range is

$$(r_{m,k})_{\text{nlos}} = d_{m,k} + n(t) + b_{m,k} \tag{11}$$

where $b_{m,k}$ are the bias because of the blocked direct path. Its magnitude of the positive bias depends on the propagation environment.

For the NLOS, range errors are normally modelled as exponential distributed. A simpler model, which models the NLOS bias as Gaussian with a positive mean, has been proposed and verified in [16]. The negative part of Gaussian with positive mean is relatively small and it is actually negligible. Assume that LOS is blocked between a blind node and an anchor node m and LOS exists between this blind node and anchor nodes k. Hence, we can model the NLOS bias as follows

$$b_{m,k} \sim N(\mu_m, \sigma^2_{\text{bias}}) \tag{12}$$

where μ_m is the positive bias of the arrival time from m to the querying node and σ^2_{bias} is the variance.

2.2 Derivation of theoretical lower bounds

CRLB is a theoretical lower bound of the variance of the position estimates and it is defined as the inverse of the FIM. $\boldsymbol{C}_{\hat{\boldsymbol{p}}}$ is the covariance matrix of the position estimator of the unknown node

$$\boldsymbol{C}_{\hat{\boldsymbol{p}}} = E[(\hat{\boldsymbol{p}} - \boldsymbol{p})(\hat{\boldsymbol{p}} - \boldsymbol{p})^{\text{T}}] \tag{13}$$

where $\boldsymbol{p} = [p_i, p_j]^{\text{T}} = [x, y]^{\text{T}}$, $E[\cdot]$ is the expected value.

$\boldsymbol{I}(\boldsymbol{p})$ represents the FIM and can be found using

$$\boldsymbol{I}(\boldsymbol{p}) = E\left[\left(\frac{\partial \ln(f(\boldsymbol{r}|\boldsymbol{p}))}{\partial \boldsymbol{p}}\right)\left(\frac{\partial \ln(f(\boldsymbol{r}|\boldsymbol{p}))}{\partial \boldsymbol{p}}\right)^{\text{T}}\right] \tag{14}$$

where $\boldsymbol{r}$ is a vector with the measured ranges as its components.

The covariance matrix and the FIM satisfy the following inequality

$$\boldsymbol{C}_{\hat{\boldsymbol{p}}} - \boldsymbol{I}^{-1}(\boldsymbol{p}) \geq 0 \tag{15}$$

We can derive that

$$(\boldsymbol{I}(\boldsymbol{p}))_{i,j} = E\left[\frac{\partial \ln(f(\boldsymbol{r}|\boldsymbol{p}))}{\partial p_i}\frac{\partial \ln(f(\boldsymbol{r}|\boldsymbol{p}))}{\partial p_j}\right] \tag{16}$$

and hence the positioning error bound satisfies

$$\sigma^2_{\text{blind}} \geq \text{tr}[\boldsymbol{I}^{-1}(\boldsymbol{p})] \tag{17}$$

where tr[·] is the trace of a square matrix, defined to be the sum of the diagonal elements.

2.2.1 DI range error case: Let M be the number of anchor nodes in the network. Anchor node with index 1 is selected as the reference anchor, which means that all TDOA ranges are measured relative to anchor node 1. Therefore we will have actual TDOA ranges $\boldsymbol{d} = [d_{2,1}, d_{3,1}, \ldots, d_{M,1}]^{\text{T}}$ and measured TDOA ranges $\boldsymbol{r} = [r_{2,1}, r_{3,1}, \ldots, r_{M,1}]^{\text{T}}$. It is assumed that all the TDOA ranges are identical and independently distributed. The DI range for TDOA measurements is modelled as Gaussian

$$\boldsymbol{r} \sim N(\boldsymbol{d}, \boldsymbol{\sigma}^2\boldsymbol{I}) \tag{18}$$

where $\boldsymbol{I}$ is the identity matrix.

doi: 10.1049/iet-smt.2010.0051

Therefore we can write the jointly conditional probability density function (pdf) function as follows

$$f(\boldsymbol{r}|\boldsymbol{p}) = \prod_{m=2}^{M} f_{m,1}(r_{m,1}|\boldsymbol{p}) = \frac{1}{(2\pi\sigma^2)^{(M-1)/2}} \exp\left[-\frac{1}{2\sigma^2}(\boldsymbol{r}-\boldsymbol{d})^{\mathrm{T}}(\boldsymbol{r}-\boldsymbol{d})\right] \quad (19)$$

As mentioned earlier, CRLB is the inverse of FIM. The bound of the variance of the blind node position can be derived as

$$\sigma^2_{\text{blind}} = \text{var}(x) + \text{var}(y) \geq \frac{(I(\boldsymbol{p}))_{11+}(I(\boldsymbol{p}))_{22}}{(I(\boldsymbol{p}))_{11}(I(\boldsymbol{p}))_{22} - (I(\boldsymbol{p}))^2_{12}} \quad (20)$$

After some mathematical manipulation, the positioning error bound can be simplified as

$$(\sigma^2_{\text{blind}})_{\text{TDOA}} \geq \frac{2\sigma^2\left(M - \sum_{m=2}^{M}\cos(\theta_{m,1})\right)}{\sum_{m=1}^{M-1}\sum_{n=2}^{M}(\sin(\theta_{m,1}) - \sin(\theta_{n,1}))^2} \quad (21)$$

where θ_i is the angle of the blind node to the anchor node i with respect to the x-axis, $\theta_{i,j} = \theta_i - \theta_j$ (Fig. 1).

2.2.2 DD range error: In the previous case, we assume that the range errors are independent of the distances between the transmitters and the receivers. That is, no matter how far away the transmitters and receivers are, the range errors are the same. However, when transmitters and receivers are placed further apart, it is reasonable that the range errors are likely to increase because of increasing reflected paths. The measurements can be modelled as

$$\boldsymbol{r} \sim N(\boldsymbol{d}, \boldsymbol{C}(\boldsymbol{p}))$$

$$\boldsymbol{C}(\boldsymbol{P}) = \begin{bmatrix} \sigma^2(d_{2,1}) & 0 & \cdots & 0 \\ 0 & \sigma^2(d_{3,1}) & \cdots & 0 \\ \vdots & \vdots & \ddots & \vdots \\ 0 & 0 & \cdots & \sigma^2(d_{M,1}) \end{bmatrix} \quad (22)$$

where $\boldsymbol{C}(\boldsymbol{p})$ is the covariance matrix of the range measurements and its elements are dependent on the distances to the querying nodes.

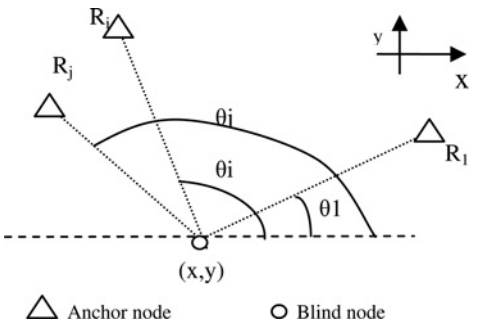

Fig. 1 *Illustration of* $\theta_{i,j} = \theta_i - \theta_j$

The FIM thus can be found using the following equation [9]

$$[\boldsymbol{I}(\boldsymbol{p})]_{i,j} = \left[\frac{\partial \boldsymbol{d}}{\partial p_i}\right]^{\mathrm{T}} \boldsymbol{C}^{-1}(\boldsymbol{p})\left[\frac{\partial \boldsymbol{d}}{\partial p_j}\right] + \frac{1}{2}\text{tr}\left[\boldsymbol{C}^{-1}(\boldsymbol{p})\frac{\partial \boldsymbol{C}(\boldsymbol{p})}{\partial p_i}\boldsymbol{C}^{-1}(\boldsymbol{p})\frac{\partial \boldsymbol{C}(\boldsymbol{p})}{\partial p_j}\right] \quad (23)$$

Since the ranges are modelled as Gaussian, the components of FIM are can be obtained by using (16) as follows

$$[\boldsymbol{I}(\boldsymbol{p})]_{1,1} = E\left[\left(\frac{\partial \ln(f(\boldsymbol{\theta}|\boldsymbol{p}))}{\partial x_{\text{i}}}\right)\left(\frac{\partial \ln(f(\boldsymbol{\theta}|\boldsymbol{p}))}{\partial x_{\text{i}}}\right)^{\mathrm{T}}\right] = \frac{1}{\sigma_0^2}\sum_{m=2}^{M}\frac{1}{d_m^{\alpha} + d_1^{\alpha}}(\cos\theta_m - \cos\theta_1)^2 + \frac{\alpha^2}{2}\sum_{m=2}^{M}\frac{1}{(d_m^{\alpha} + d_1^{\alpha})^2}(d_m^{\alpha-2}\cos\theta_m - d_1^{\alpha-2}\cos\theta_1)^2 \quad (24)$$

The other components of the FIM can be derived in the same way. The CRLB for DD can be obtained simply by substituting these components into (20).

2.2.3 NLOS bias: NLOS error is the dominant error in location estimation. Assume that only γ out of M anchor nodes have direct LOSs to the querying nodes. In Section 2.1, the bias due to blocking of LOS is modelled as Gaussian with a positive mean. Generally, NLOS range measurements have a larger variance than LOS range measurements. This feature has also been used in some algorithms to identify LOS and NLOS measurements. Assuming that the Gaussian measurement noise has zero mean and variance σ^2_{noise}, the sum of NLOS bias and the measurement noise is also a Gaussian random variable with mean μ_{bias} and variance $\sigma^2_{\text{noise}} + \sigma^2_{\text{bias}}$. In this case, the joint pdf is the product of the LOS components and NLOS components

$$f(\boldsymbol{r}|\boldsymbol{p}) = \prod_{m=2}^{M} f_{m,1}(r_{m,1}|\boldsymbol{p}) = \underbrace{\prod_{m=2}^{\gamma} f_{m,1}(r_{m,1}|\boldsymbol{p})}_{f_{\text{los}}(\boldsymbol{r}|\boldsymbol{p})} * \underbrace{\prod_{n=\gamma+1}^{M} f_{n,1}(r_{n,1}|\boldsymbol{p})}_{f_{\text{nlos}}(\boldsymbol{r}|\boldsymbol{p})} \quad (25)$$

The range errors for LOS measurements are Gaussian with zero mean and covariance matrix $\boldsymbol{C}_{\text{los}}(\boldsymbol{p})$, whereas the range errors for NLOS measurements are also Gaussian with mean $\boldsymbol{u}$ and covariance matrix $\boldsymbol{C}_{\text{nlos}}(\boldsymbol{p})$.

$$\boldsymbol{C}_{\text{los}}(\boldsymbol{p}) = \text{diag}[\sigma^2_{\text{los}}(d_{2,1}), \ldots, \sigma^2_{\text{los}}(d_{\gamma,1})] \quad (26)$$

$$\boldsymbol{C}_{\text{nlos}}(\boldsymbol{p}) = \text{diag}[\sigma^2_{\text{nlos}}(d_{\gamma+1,1}), \ldots, \sigma^2_{\text{nlos}}(d_{M,1})] \quad (27)$$

For the NLOS case, we can obtain the components of the FIM

using (27)

$$
\begin{aligned}
[\boldsymbol{I}(\boldsymbol{p})]_{i,j} &= E\left[\frac{\partial \ln(f(\boldsymbol{r}|\boldsymbol{p}))}{\partial p_i}\frac{\partial \ln(f(\boldsymbol{r}|\boldsymbol{p}))}{\partial p_j}\right] \\
&= E\left[\frac{\partial \ln(f_{\text{los}}(\boldsymbol{r}|\boldsymbol{p}))}{\partial p_i}\frac{\partial \ln(f_{\text{los}}(\boldsymbol{r}|\boldsymbol{p}))}{\partial p_j}\right. \\
&\quad + \frac{\partial \ln(f_{\text{nlos}}(\boldsymbol{r}|\boldsymbol{p}))}{\partial p_i}\frac{\partial \ln(f_{\text{nlos}}(\boldsymbol{r}|\boldsymbol{p}))}{\partial p_j} \\
&\quad + \frac{\partial \ln(f_{\text{los}}(\boldsymbol{r}|\boldsymbol{p}))}{\partial p_i}\frac{\partial \ln(f_{\text{nlos}}(\boldsymbol{r}|\boldsymbol{p}))}{\partial p_j} \\
&\quad \left. + \frac{\partial \ln(f_{\text{nlos}}(\boldsymbol{r}|\boldsymbol{p}))}{\partial p_i}\frac{\partial \ln(f_{\text{los}}(\boldsymbol{r}|\boldsymbol{p}))}{\partial p_j}\right] \\
&= E\left[\frac{\partial \ln(f_{\text{los}}(\boldsymbol{r}|\boldsymbol{p}))}{\partial p_i}\frac{\partial \ln(f_{\text{los}}(\boldsymbol{r}|\boldsymbol{p}))}{\partial p_j}\right. \\
&\quad \left. + \frac{\partial \ln(f_{\text{nlos}}(\boldsymbol{r}|\boldsymbol{p}))}{\partial p_i}\frac{\partial \ln(f_{\text{nlos}}(\boldsymbol{r}|\boldsymbol{p}))}{\partial p_j}\right] \qquad (28)
\end{aligned}
$$

CRLB for NLOS can then be derived using the similar steps as in the previous two cases. The results derived above are not limited to UWB ranging. However, only UWB ranging can guarantee high accuracy in multipath environments.

3 Numerical results

3.1 Examples of fundamental localisation limits

The section provides some examples of the derived fundamental limits. Fig. 2 shows the examples of CRLB for three cases: case (i) DI range error, case (ii) DD range error and case (iii) NLOS. The interested area is a 40 m × 40 m square with its centre located at the coordinate of (0, 0). Five anchor nodes are evenly located in a unit circle. Anchor node 1 acts as the referencing node with coordinate (15, 0). The standard deviation of the measurement noise is chosen as 0.1 m. Although the standard deviation is less than 0.1 m from our UWB range measurement [12], 0.1 m is chosen just for simplicity and easy illustration. It can be observed that lower theoretical positioning errors are inside the convex hull for all the three cases. To illustrate the positioning error distribution pattern more clearly, line $x = 0$ and $y = 0$ is used to 'cut' the contour plots in Fig. 2, and the curves for $M = 5$ are shown in Fig. 3.

Case (i): All the terms in (21) are dimensionless, which indicates that the theoretical bound for case (i) is independent of the dimension of the network if the range errors are independent of the distance. Furthermore, the lower bound is actually proportional with the standard deviation, that is, the positioning error increases proportionally with the standard deviation. However, the error is independent of the actual size of the network as long as the ranging errors are zero-mean Gaussian distributed, and hence the pattern for the theoretical bound remains the same. It can be observed from (21) that the CRLB bound depends on the angles between the blind node and anchor nodes, that is, the geometry of the network.

Case (ii): Substituting (24) and other FIM components into (20), the distance terms cannot be eliminated as (21), which indicates that the positioning accuracy is no longer dimension independent, although it relies not only on the geometry but also on the size of the network. The minimum value is closer to the TDOA referencing node, anchor node 1. Comparing Fig. 2*b* with Fig. 2*a*, it is obvious that case (i) has much lower minimum values. This result is reasonable since the TDOA ranges accuracy degrades exponentially with the distances, and hence worsens the position estimate results.

Case (iii): It is assumed that the blind node has no LOS to anchor node 4, $(15\cos(8\pi/5), 15\sin(8\pi/5))$, for example, there is an obstacle located very close to anchor node 4. Observing Figs. 2*b* and *c*, it can be found that there is an abrupt change of positioning accuracy around anchor node 4. This is because the ranges to that node are no longer reliable. However, ranges with small NLOS errors will have better positioning accuracy than positioning with the NLOS ranges [12]. The minimum value is no longer close to anchor node 1 as in cases (i) and (ii).

3.2 Experimental campaign

3.2.1 Experiment setup: Experimental campaign was conducted to investigate the performance of UWB TDOA localisation in a typical indoor environment Fig. 4 illustrates

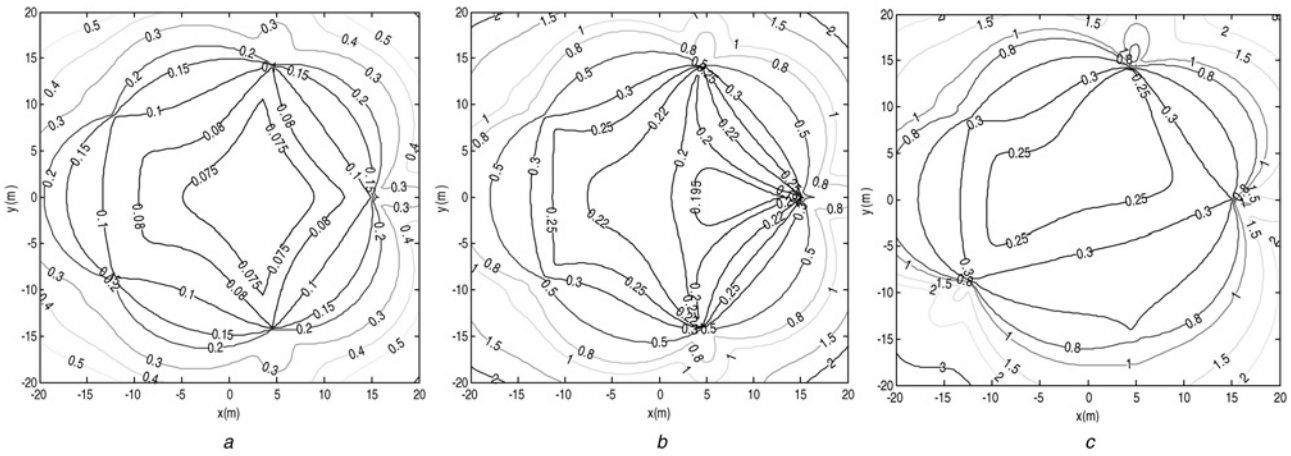

Fig. 2 *Contour plot of CRLB for TDOA*

a DI range error, $\sigma = 0.1$ m
b DD range error, $\alpha = 0.5$, $\sigma_0 = 0.1$ m
c NLOS bias, $\alpha = 0.5$, $\sigma_0 = 0.1$ m, $\sigma_{\text{bias}} = 1$ m

doi: 10.1049/iet-smt.2010.0051

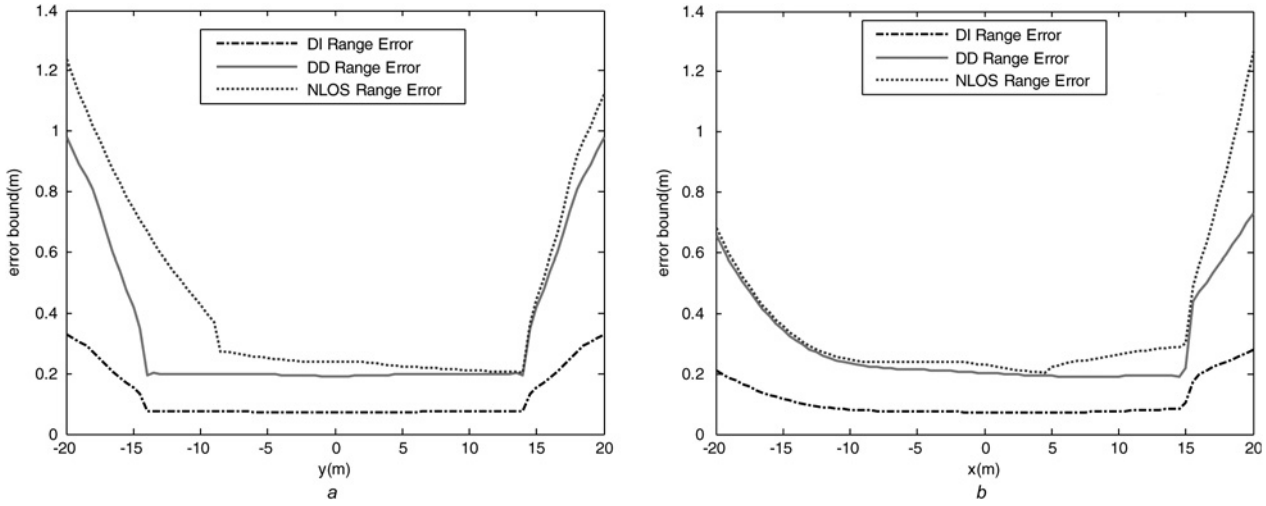

Fig. 3 *Comparison of CRLB for TDOA DD, DI and NLOS cases*
a $x = 0$
b $y = 0$

our experimental set-up which consists of three receivers and one transmitter. Three receivers acting as anchor nodes are placed at known positions, whereas the transmitter or blind node is mobile and its position is to be determined. The transmitted UWB pulse from the blind node arrives at the three antennas of the anchor nodes at different times. The difference on signal arrival time can be easily obtained. The Gaussian pulse generator, which is triggered by the 10 MHz clock, generates a UWB pulse with centre frequency around 4 GHz. A power amplifier is then used and the output signal is emitted through an asymmetrical biconical antenna. All the antennas are mounted on wooden sticks with height of 1.25 m. The receivers also use the biconical antennas. The received UWB signals after the antenna are amplified by a low-noise amplifier (LNA) before being sampled by an Agilent oscilloscope. The oscilloscope can synchronise the acquisitions received from the three receivers and hence the TDOA information can be obtained.

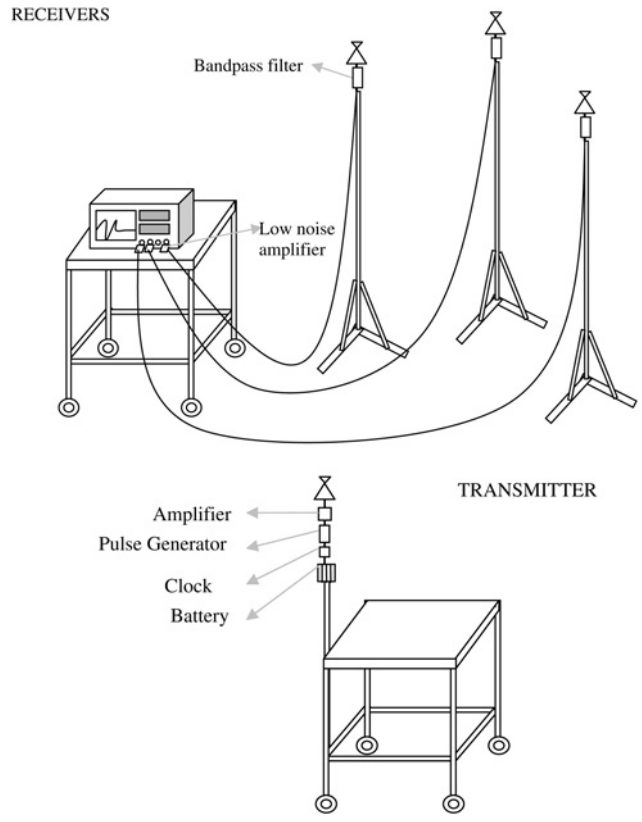

Fig. 4 *Experimental set-up for TDOA measurement*

3.2.2 Range measurements: The measurements aim to find the differences of the TOA of the signals from the transmitter to the three receivers whose locations are known. Each range difference determines a hyperbola, and the intersection point of the two hyperbolas is the estimated location of the querying node. For each receiver, the relative TOA is determined by applying correlation between the received signal and the template signal. In the experiments, we observe and discuss three different cases. LOS propagation is necessary for accurate range estimation. If there is no LOS between two nodes, the UWB pulse will travel an extra distance and hence extra time of propagation. NLOS error is the dominant error in the range estimation. NLOS situation can be further divided into two cases: absolute blockage and partial blockage (Fig. 5). In the first case, one receiver is totally blocked, and the UWB signals can only penetrate through the obstacle. Obviously, the signals will travel longer time through the obstacle as the radio speed is slower in other material than that in the air. In the latter case, the received signal is a combination of the signals travelling through obstacle and those reflected from the wall or other obstacles and again a positive bias will be introduced into the range errors. A grid system has been used in the measurement with 121 sets of TDOA ranges from the transmitters to the receivers measured.

As mentioned earlier, UWB signals can provide a high time resolution. Therefore obtaining the time delay because of the cable becomes crucial. In the measurement campaign, we measured the time difference instead of absolute time, and hence it is sufficient to find the relative cable delay. We can obtain the cable delay by following the procedure: one transmitter is placed in the middle of the two receivers to find the offset of the two pulse peaks. The offset is used to compensate the time delay because of the subminiature version A (SMA) cables.

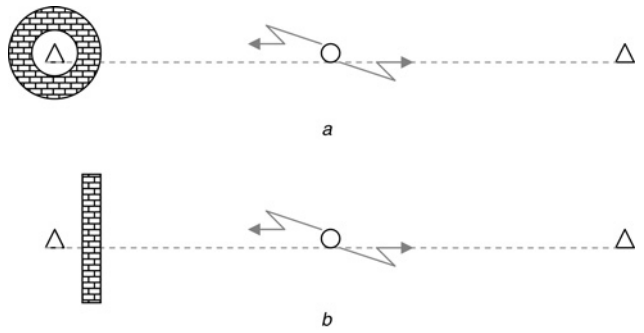

Fig. 5 *NLOS environment*

a Absolute blockage
B Partial blockage

The LOS measurements were conducted in the entrance hall of the Research Technoplaza, Nanyang Technological University. The receivers were placed at fixed locations and the distance between them was 12 m. All the receivers had LOS to the transmitter. The transmitter is moved within a 15 m × 15 m rectangular area which has the triangle formed by the three receivers at its centre.

A straightforward TDOA estimate between a pair of antennas can be obtained by finding the peak of the cross correlation function. The performance of conventional correlator and various phase-only correlators have been discussed in [17]. Fig. 6 shows one example of the time difference in the pulse peaks. The offset between pulse peaks for anchor nodes 1 and 2 is around 5.55 ns which gives 1.665 m range difference. From the TDOA range data, we can calculate the range errors from the known actual positions of both transmitter and receiver and thus derive the statistical model for the range error ε. The pdf can be obtained by fitting the histogram and expressed in a mathematical form as a Gaussian distribution function

$$f(\varepsilon) = \frac{1}{\sqrt{2\pi\sigma^2}} \exp\left(-\frac{(\varepsilon - \bar{\varepsilon})^2}{2\sigma^2}\right) \tag{29}$$

where $\bar{\varepsilon} \simeq 0.0058$ m, which can been seen as zero mean with the standard deviation is $\sigma \simeq 0.0477$ m. The range errors are resulted from measurement noise.

The NLOS-total blockage measurements for NLOS cases were conducted inside positioning and wireless technology centre, a typical indoor environment. One receiver is placed behind a concrete wall, whereas the other two receivers have LOS to the transmitter. The NLOS range errors are normally modelled as exponential distributed. However, a simple way to model it is to use the Gaussian distribution. A simpler model based on UWB indoor measurements is proposed where the NLOS bias is modelled as Gaussian with a positive mean. Similar to the LOS case, the corresponding pdf can be obtained by fitting the histogram

$$f(\varepsilon) = \frac{1}{\sqrt{2\pi\sigma^2}} \exp\left(-\frac{(\varepsilon - \bar{\varepsilon})^2}{2\sigma^2}\right) \tag{30}$$

where $\bar{\varepsilon} \simeq 0.3901$ m, which is the mean of the pdf function and the standard deviation is $\sigma \simeq 0.0679$ m.

To test the attenuation because of the wall, we put the transmitter in the centre between two receivers, one behind the concrete wall and one at the same side as the transmitter. The time difference of the arrival pulses should be zero if there is no wall between the two receivers. A bias will appear when the concrete wall exists, and the time difference is found to be 1.365 ns which corresponds to 0.4095 m in distance. This result is close to the mean of (30) $\bar{\varepsilon} \simeq 0.3901$ m . It has been found in (29) that the LOS Gaussian pdf is nearly zero mean, and therefore the positive mean here can be seen as the attenuation because of the wall. The situation is more challenge for NLOS-partial blockage case, because the received signals include the multipath signals and the signals through obstacle. The direct-path signal is not always the strongest one because of the higher attenuation through material propagation. It is necessary to be able to detect the first arrival signal.

3.2.3 Position estimation using measured ranges:

To estimate the positions of the blind nodes, we can simply compare the measured ranges and those computed from the node coordinates, and minimise the differences [8]. The

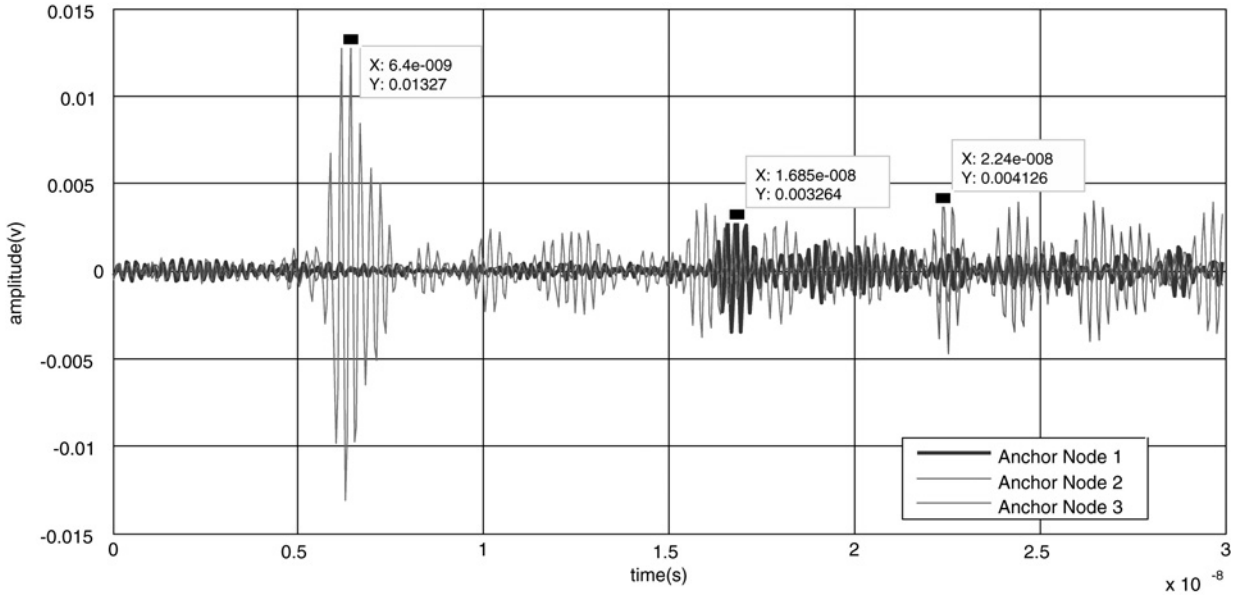

Fig. 6 *Pulses received at three anchor nodes and the offset of the pulse peaks gives the time difference*

doi: 10.1049/iet-smt.2010.0051

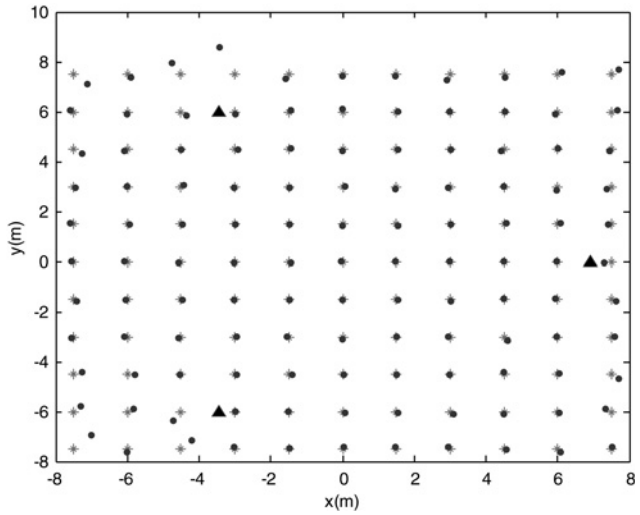

Fig. 7 *Estimated locations (dots) against actual locations (stars)*
Triangles are the anchor nodes. The locations enclosed by dotted area have relatively large positioning error

performance of the positioning method can be measured using root mean square error (RMSE), which is obtained by comparing estimated positions with actual positions. Lower RMSE means better performance.

After obtaining the ranges from the transmitter to the receivers, the position of the transmitter can be estimated by minimising the following cost function (31). The conjugate gradient method can be used to carry out the minimisation [18]

$$F(\boldsymbol{p}) = \sum_{m=2}^{M} (||\boldsymbol{p} - \boldsymbol{p_m}|| - ||\boldsymbol{p} - \boldsymbol{p_1}|| - r_{m,1})^2 \qquad (31)$$

where M is the number of anchor nodes, and $\boldsymbol{p} = [x, y]^{\mathrm{T}}$, $r_{m,1}$ is the TDOA range from receiver m and 1 to the transmitter.

Here, we want to find all the estimated positions of the transmitters being placed, and the following cost function can be employed

$$F(\boldsymbol{p}_1, \boldsymbol{p}_2, \ldots, \boldsymbol{p}_N) = \sum_{k=1}^{N} \sum_{m=2}^{M} (||\boldsymbol{p}_k - \boldsymbol{p}_m|| - ||\boldsymbol{p}_k - \boldsymbol{p_1}|| - r_{m,1})^2 \qquad (32)$$

where N is the total number of locations of the transmitters being placed.

Fig. 7 shows a comparison of the actual node locations with the estimated node locations. It can be observed that the positioning errors within the triangular area which is formed by the three receivers are relatively smaller compared to those locations outside the area, especially those nodes close to the receiver. We measure the performance of the positioning method with RMSE, which is obtained by comparing estimated positions with actual positions. The RMSE for LOS and NLOS are found to be 0.0811 and 0.1082 m, respectively.

4 Conclusion

The closed-form expressions of CRLB have been derived for TDOA UWB positioning for both LOS and NLOS environments. Moreover, the theoretical analysis has been proved by the measurement results obtained from real experiments. Based on the analysis and experiments, it has been investigated how the number of anchor nodes and the geometry of the network affect the positioning accuracy. It is found that the lower positioning errors appear in the convex hull formed by the anchor nodes for the positioning. However, the minimum value is no longer in the centre area for the positioning with DD errors. The derived expressions have also revealed that the lower bound for the case with DD range errors is relevant to the actual dimension of the network. With the same anchor node placement, a larger network will have worse localisation performance because the ranging accuracy degrades exponentially with the distance.

5 References

1 Fontana, R.J.: 'Recent system applications of short-pulse ultra-wideband (UWB) technology', *IEEE Trans. Microw. Theory Tech.*, 2004, **52**, (9), pp. 2087–2104
2 Win, M.Z., Scholtz, R.A.: 'Impulse radio: how it works', *IEEE Commun. Lett.*, 1998, **2**, (2), pp. 36–38
3 Fontana, R.J., Gunderson, S.J.: 'Ultra-wideband precision asset location system'. IEEE Conf. on Ultra Wideband Systems and Technologies, 21–23 May 2002, pp. 147–150
4 Gezici, S., Tian Z., Giannakis, G.B., *et al.*: 'Localization via ultra-wideband radios: a look at positioning aspects for future sensor networks', *IEEE Signal Process. Mag.*, 2005, **22**, (4), pp. 70–84
5 Chung, W.C., Ha, D.S.: 'An accurate ultra wideband (UWB) ranging for precision asset location'. Proc. IEEE Conf. on Ultra Wideband Systems and Technologies, November 2003
6 Chan, Y., Ho, K.C.: 'A simple and efficient estimator for hyperbolic location', *IEEE Trans. Signal Process.*, 1994, **42**, (8), pp. 1905–1915
7 Patwari, N., Hero, A.O., Perkins, M., Correal, N.S., O'Dea, R.J.: 'Relative location estimation in wireless sensor networks', *IEEE Trans. Signal Process.*, 2003, **51**, (8), pp. 2137–2148
8 Xu, J., Ma, M., Law, C.L.: 'Position estimation using ultra-wideband time difference of arrival measurements', *IET Sci. Meas. Technol.*, 2008, **2**, (1), pp. 53–58
9 Foy, W.H.: 'Position-location solutions by Taylor-series estimation', *IEEE Trans. Aerosp. Electron. Syst.*, 1976, **AES-12**, (2), pp. 187–194
10 Steven, M.K.: 'Fundamentals of statistical signal processing: estimation theory' (Prentice Hall, Englewood Cliff, NJ, USA, 1993)
11 Xu, J., Ma, M., Law, C.L.: 'Theoretical lower bound for UWB TDOA positioning'. IEEE GLOBECOM '07, 26–30 November 2007, pp. 4101–4105
12 Chang, C., Sahai, A.: 'Estimation bounds for localisation'. First Annual IEEE Communications Society Conf. on Sensor and Ad Hoc Communications and Networks Sensor and Ad Hoc Communications and Networks, 2004, pp. 415–424
13 Qi, Y., Kobayashi, H.: 'Cramer–Rao lower bound for geolocation in non-line-of-sight environment'. IEEE Proc. Int. Conf. on Acoustics, Speech, and Signal Processing, 2002 (ICASSP '02), 13–17 May 2002, vol. 3, pp. 2473–2476
14 Shen, Y., Wymeersch, H., Win, M.Z.: 'Fundamental limits of wideband cooperative localization via Fisher information'. IEEE Wireless Communications and Networking Conference, 11–15 March 2007, pp. 3951–3955
15 Jourdan, D.B., Dardari, D., Win, M.Z.: 'Position error bound for UWB localisation in dense cluttered environments', *IEEE Trans. Aerosp. Electron. Syst.*, 2008, **44**, (2), pp. 613–628
16 Alavi, B., Pahlavan, K.: 'Modelling of the TOA-based distance measurement error using UWB indoor radio measurements', *IEEE Commun. Lett.*, 2006, **10**, (4), pp. 275–277
17 Win, M., Scholtz, R.: 'On the performance of ultra wide bandwidth signals in dense multipath environment', *IEEE Commun. Lett.*, 1998, **2**, (2), pp. 51–53
18 Press, W.H., Flannery, B.P., Teukolsky, S.A., Vetterling, W.T.: 'Numerical recipes in C: the art of scientific computing' (Cambridge University Press, 1993)